Online, In-Situ Calibration of Underwater Hydraulic Manipulators Using a Wrist-Mounted Camera

Amy Phung
Olin College of Engineering
Summer 2020

Abstract

Hydraulic manipulator arms are commonly used for a variety of underwater tasks requiring a high degree of both strength and dexterity, ranging from scientific tasks such as capturing delicate live organisms or sampling hydrothermal vent fluids to maintenance tasks including pipeline and dam inspection. Accurately knowing the position and orientation of a manipulator's end effector with respect to objects in its environment is essential for automating manipulation, which is key for increasing both the range and complexity of sampling or maintenance tasks. While a lot of prior work has been completed in this space, the need remains for a calibration process to characterize the relationship between raw feedback from joint angle sensors and actual manipulator joint angles - particularly in situations where this relationship is dynamic and needs to be calibrated in remote environments.

In this work, we propose two different calibration methods to simultaneously compute the joint sensor offset and gains for a 6 degree-of-freedom manipulator based on input from a calibrated wrist-mounted camera. The accuracy and robustness to different levels of measurement uncertainty are analyzed for both methods and are presented in this report.

Background

Context
Manipulator arms are a common solution to completing dexterous tasks, especially when completing such tasks require enduring harsh environmental conditions or demand for significant physical strength. In the marine sciences space, hydraulic manipulator arms are often installed on deep submergence vehicles [1] like the HROV Nereid Under Ice [2], the DSV Alvin, or the ROV Jason [3] to collect samples critical to forwarding our understanding of the Earth's oceans. Whether it's capturing delicate live organisms [4] [5] [6], sampling hydrothermal vent fluids [7], or using a suction sampler to collect microbes in environments [6], these tasks require dexterity in depths far deeper than scuba divers can operate in. However difficult, it's important to find a means of collecting these samples since they can provide us with a wealth of information ranging from impacts of natural disasters to new sources of widely used minerals scarce in terrestrial environments.

Although the importance of studying the world's oceans cannot be understated, more than eighty percent of our ocean remains unexplored [8]. This is likely attributed to the fact that operating in deep-sea environments poses a unique set of challenging environmental factors, including but not limited to extreme pressures [9], scattering of light [5], and a wide range of temperatures. This environment also poses some technological challenges such as limited bandwidth for communication, inability for physical human intervention, and limited power for lighting and computation; thus, a high degree of autonomy when operating in such environments is critical. Overcoming these challenging conditions will also get us one step closer to studying oceans on other planetary bodies like Europa and Enceladus, both of which have large oceans below a deep layer of ice that are of significant scientific interest [10].

Manipulator Calibration

In order to automate complex manipulation tasks, a manipulator typically requires calibration in order to locate the position of its end effector with respect to objects within its environment. In general, manipulator calibration can be broadly categorized into three levels as proposed by Mooring et al. [11]:

1. "joint level" calibration, which determines the relationship between the raw joint sensor signal and the actual joint angles
2. "kinematic model" calibration, which determines the basic kinematic geometry of the robot as well as the correct joint-angle relationships
3. "non-kinematic" calibration, which is correcting for the effects of non-geometric errors such as joint and link compliance, friction, and gear backlash

The methods presented in this study will focus on "joint level" calibration since accurate knowledge of the manipulator's joint angles is a prerequisite for higher levels of calibration.

Common joint angle sensors used in manipulators include encoders and potentiometers, which produce a digital signal or analog voltage based on rotary or linear motion. In conventional cases, the functional relationship between the signal from the sensor η and the actual joint angle θ is assumed to be linear and can be written as: [11]

$$\theta = k_1 \eta + k_2$$

Where k_1 is the joint position sensor gain (joint angle represented by each unit change of the sensor) and k_2 is joint angle offset (the joint angle when the sensor reading is 0)

Prior Level 1 Calibration Techniques - Encoders

In the case of encoders, the ratio between the changes in sensor measurements and actual joint angles k_1 (joint position sensor gain) can be determined by "simply obtaining the number of lines on the encoder and checking to see if the electronic counter in the controller multiplies the count by 1, 2, or 4" [11]. Although this process alone is typically sufficient for encoders, Švaco et al. [12] included a joint sensor gain for each of the joints as additional parameters to correct for slight errors that result from this process. Calibration of the joint angle offsets k_2 is a

bit more complicated, and various calibration processes have been developed to complete this calibration given that the sensor gain is known. Previous work in this space will be discussed in this section.

One popular approach commonly used in industrial applications involves pointing a laser pointer mounted on the end-effector at a position sensitive device in the workspace from a variety of positions [13] [14] [15]. Chen et al. [16] proposed an approach similar to this, except that the laser is mounted in the workspace and the manipulator is manually moved such that a specific point on the end-effector is in-line with the laser. Other approaches required an external laser tracker and measuring a circular trajectory by rotating each joint individually through its full range of motion [17] [18]. Zhuang et al. [19] proved that 3 plane constraints were required to calibrate a manipulator arm, which has been used to improve calibration of kinematic parameters for a 6-DoF manipulator and the extrinsic parameters of a 2D laser attached to the end effector [20]. Lind [21] proposed a contact-based calibration method that uses a wrist-mounted force sensor, calibration probe, and a calibration plate. Contactless camera-based calibration approaches are also commonly used in industrial settings [22] [12].

In cases where relying on external sensors mounted in the workspace is not feasible, as would be the case with most mobile robots, gravity-based approaches have been proposed. One involves placing two accelerometers on adjacent links to estimate the joint angles directly and it is currently used on heavy-duty mining shovels [23]. Similar approaches use inertial measurement units to directly estimate joint angles [24] [25] [26]. While these sensing methods don't replace resolvers, encoders, or other contact-based angle sensors, the results aren’t reliant on encoders and can be used for fault detection or as a backup angle measurement system.

In addition to calibrating joint angle offsets during calibration, other methods involved techniques to simultaneously calibrate intrinsics and extrinsics of other sensors, such as the bundle adjustment approach proposed by Pradeep et al. [27] and the joint calibration approach proposed by Le and Ng [28]. This approach has been used to fully calibrate robots with manipulator arms and cameras, such as the single-armed Fetch robot and the two-armed JANUS robot prototype [29] [30].

Although these calibration processes work well for calibrating encoders, they’re not immediately extensible to calibrating potentiometer output due to their implicit assumption that the joint sensor gain is known before calibration. Calibration techniques for potentiometers are discussed in the next section.

Prior Level 1 Calibration Techniques - Potentiometers

Although linear potentiometers tend to have problems with low precision that reduces their popularity for measuring joint angles [11], they’re widely used in hydraulic underwater manipulators [1] due to their better tolerance for extreme pressures. However, because of analog electronics associated with the use of potentiometers, the need for periodic recalibration

of joint angle offsets and ratios has been documented [31] It's also worth noting that potentiometer measurements tend to be dependent on temperature and pressure, especially in underwater environments where pressures can reach 16,000 PSI [32] and temperatures range from -2°C to 30°C [33]. To accurately characterize the potentiometer to angle relationship in a lab setting, the manipulator would need to be placed in a controlled environment that replicated these conditions. This would be extremely expensive and time-consuming, and would also need to be done regularly due to the fact that the potentiometers naturally experience some drift over time. It would be much more practical to develop a calibration process that can be completed in the field, which is what this study aims to address.

Some prior studies discuss various methods for calibrating the joints' potentiometer to angle relationships. Williams [34] proposed computing this relationship by recording the potentiometer outputs by driving each joint to its two nominal limits, and then using a general linear calibration equation that finds both the joint angle offset and scaling terms. He does note that the calibration could be improved by taking multiple measurements and then using a linear least-squares fit to compute the relationship, but ultimately concluded that the proposed calibration was sufficiently accurate for his application. Wu et al. [35] noted that manual calibration approaches typically rely on using protractors and rulers to get a ground-truth joint angle measurement, and suffered from inaccuracies and inefficiencies when applied to complex robots. They proposed an automated method using 24 optical markers for motion capture placed on a 36 DoF humanoid to calibrate joint potentiometers, tendon length sensors, and the motion capture marker positions on the robot. A gravity-based approach using joint torque sensors proposed by Ma et al. [36] leveraged the fact that the torque exerted on each joint by gravity varies sinusoidally with the rotation angle to calibrate joint sensor offsets and gains.

Limitations

To our knowledge, the current methods of joint sensor calibration are not extensible to our application of calibrating potentiometer-based hydraulic manipulator arms installed on deep submergence vehicles. Due to physical constraints imposed by a particular vehicle's geometry, driving the arm to nominal limits as Williams proposed is often not possible. This approach also does not accommodate obstacles that may obstruct the arm's path, which is an important consideration for manipulators operating in the field. Using motion capture markers would require a stable external camera with a good view of the arm during calibration, which is a difficult perspective to get on board a mobile underwater platform. A gravity-based approach with joint torque sensors is not ideal on board a mobile vehicle that experiences some rotation along all three orientation axes during calibration. Falling back to a manual calibration approach with protractors and rulers is also not possible since operators cannot approach depths at which the arms operate at, and the calibration must be completed in-situ due to the effects of temperature and pressure on analog components like potentiometers. These factors highlight a need for the calibration approach proposed in this paper.

Our Approach

Our calibration method relies on measurements from a wrist mounted camera observing fiducials in the environment around the manipulator. The position of one fiducial mounted on the base of the manipulator arm needs to be known before calibration. However, keeping the one base fiducial in view of the camera at all times would prevent sufficient excitation of the joints in the calibration dataset, likely leading to poor results. To combat this, we rely on TagSLAM [37] to provide an accurate transform between each of the fiducials placed in the environment and the base fiducials. This way, we can treat all of the fiducials as landmarks with known positions opposed to just the one base fiducial.

After observing the fiducials, we can re-project these observations through the kinematic chain of the arm to estimate their positions based on the hypothesized joint angle parameters, similar to the approaches used in [29] and [27]. However, unlike those approaches, we also include the joint sensor gain for each joint as additional free parameters to the system. We then optimize the system by finding a set of parameters that minimizes the distances between the fiducials' estimated positions and their actual position.

This method can be employed to characterize linear relationships between any joint angle sensor and the actual joint angles, whether it's calibrating the mapping of potentiometers, encoders, or an unknown gear ratio between the sensors and the joint angle. The contribution of this work is a novel method to calibrate the ratio between the raw sensor output and joint angles that can be completed with a wrist mounted camera without an operator physically present. Experimental and simulated results from implementing our method on a hydraulic Kraft manipulator arm are presented.

Minimum Variance Method

Kim et al. [38] proposed using the minimum variance method for robot head-eye calibration, and we extended their implementation to include the joint offset and scaling terms as additional free parameters in the objective function. When using this method, the only requirement is that the observed landmark is stationary. Although this method seems appealing since it doesn't require the position of the observed landmark to be known, we found that it is not a robust solution to our problem due to its sensitivity to measurement noise. This section will explain the analysis that informed this conclusion.

The core concept behind this method is that if all of the free parameters are correct, transforming observations of the same landmark from the wrist camera to the root link from a variety of arm positions should result in the same point in the root link frame. However, if the parameters are incorrect, the observations will appear to be disjointed when this transformation is applied. Because of this, we can construct an objective function that aims to minimize the variance between observations of the same landmark in the base frame.

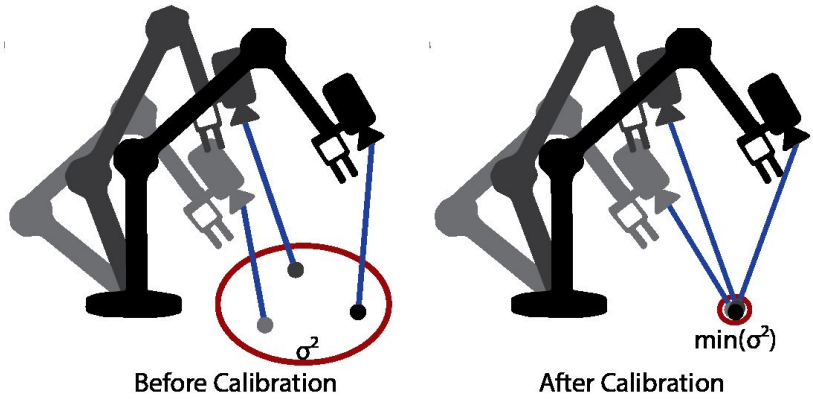

Figure 1: Minimum variance method visualization - the minimum variance method minimizes the variance of the reprojected observations of the same landmark in the base frame

Objective Function

We can apply equation 1 to describe each of the sensor to angle relationships for individual joints. For a particular joint i, this would be

$$\theta_i = k_{i1}\eta_i + k_{i2}$$

After vectorizing this relationship to include all of the joints in the manipulator, we get

$$\boldsymbol{\theta} = \mathbf{k}_1\boldsymbol{\eta} + \mathbf{k}_2$$

The free parameters of the system to be optimized include the joint gain and offset variables, which can be written as

$$\mathbf{v} = \begin{bmatrix}\mathbf{k}_1 & \mathbf{k}_2\end{bmatrix}$$

Additional definitions of notation are clarified below:

${}^{b}\mathbf{z}_{ij}$: 3D position of the ith measurement of landmark j in the base frame

${}^{c}\mathbf{z}_{ij}$: 3D position of the ith measurement of landmark j in the camera frame

${}^{c}\mathbf{z}_{j}$: measurements of landmark j in the camera frame

${}^{b}\boldsymbol{\mu}_{j}$: the average 3D position of measurements in the base frame for landmark j

${}^{b}\mu_{j_x}$: The average value of the x component of measurements in the base frame for landmark j

Each calibration data point ${}^{c}\mathbf{z}_{ij}$ is a 3D position of an observed landmark j with respect to the wrist camera frame. By using the forward kinematics and the joint angle gains $\mathbf{k}_1$ and offsets $\mathbf{k}_2$, we can compute the estimated position of the calibration point with respect to the base frame ${}^{b}\mathbf{z}_{ij}$. The covariance matrix is then computed for each landmark using the equation:

$$
\begin{aligned}
C_{j_{xx}} &= E\left[\left({}^{b}\mathbf{z}_{j_x} - {}^{b}\mu_{j_x}\right)\left({}^{b}\mathbf{z}_{j_x} - {}^{b}\mu_{j_x}\right)\right] \\
C_{j_{xy}} &= E\left[\left({}^{b}\mathbf{z}_{j_x} - {}^{b}\mu_{j_x}\right)\left({}^{b}\mathbf{z}_{j_y} - {}^{b}\mu_{j_y}\right)\right] \\
&\vdots \\
C_{j_{zz}} &= E\left[\left({}^{b}\mathbf{z}_{j_z} - {}^{b}\mu_{j_z}\right)\left({}^{b}\mathbf{z}_{j_z} - {}^{b}\mu_{j_z}\right)\right]
\end{aligned}
$$

$$
\Sigma_j = \begin{bmatrix} C_{j_{xx}} & C_{j_{xy}} & C_{j_{xz}} \\ C_{j_{yx}} & C_{j_{yy}} & C_{j_{yz}} \\ C_{j_{zx}} & C_{j_{zy}} & C_{j_{zz}} \end{bmatrix} \left(\text{ for } j = 1 \cdots n\right)
$$

where n is the number of landmarks

From this covariance matrix, we can, we compute the total amount of variance in the set of transformed points for each landmark by using the eigenvalues. Since eigenvalues represent the variance in the variables in a particular direction, the total variance of the dataset along all three dimensions can be computed from a sum of eigenvalues along each of the x,y, and z axes.

Since the sum of eigenvalues is equal to the trace of the covariance matrix, our objective function can be represented by the equation:

$$
\mathbf{v}^{\star} = \arg\min_{\mathbf{v}} \left(\sum_{j=1}^{n} (C_{j_{xx}} + C_{j_{yy}} + C_{j_{zz}}) \right)
$$

In other words, the solution to this optimization problem is the set of free parameters $\mathbf{v}^{\star}$ that would minimize the eigenvalue sum of the covariance matrix, and thus would minimize the variance of the measurements when transformed to the base frame.

Like the method proposed by Kim et al. [38], we use the BOBYQA algorithm for bound constrained optimization proposed by Powell since it's a derivative-free method that handles noisy data relatively well.

Preconditioning
Like other optimizers, the BOBYQA algorithm converges to more accurate solutions in fewer iterations if the initial parameters are preconditioned. In our case, raw joint feedback can come in many ranges, which can cause issues during optimization. For example, a 16 bit encoder's raw output will be in the range of 0 to 65,536, while the desired output in radians may range from $-\pi$ to π. In this situation, the free parameters for the scaling terms will require

adjustments typically in the thousands range while the joint angle offsets will never require adjustments greater than 2π. The BOBYQA algorithm struggles to find good solutions when both of these parameters need adjustments that differ by several orders of magnitude, as illustrated by Figure 2. To improve the quality of our results, all of our parameters are re-scaled by the initial level of uncertainty so that they all require approximately the same magnitude of adjustment.

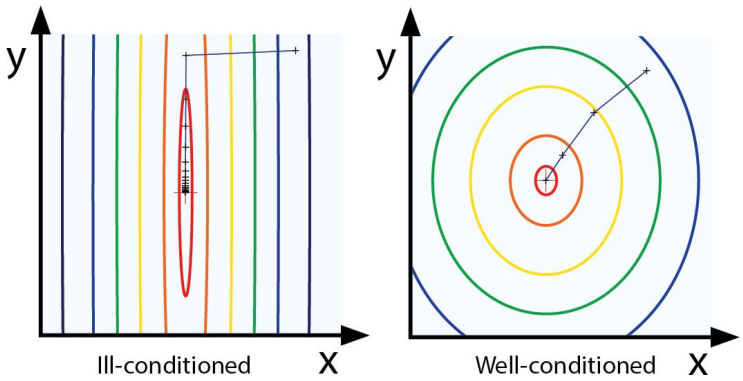

Figure 2: It's much easier for optimizers to solve well-conditioned problems like the second one than ill-conditioned problems like the first one. Since we typically know the uncertainty levels in our measurements, we can rescale our parameters before running the optimizer.

Analysis & Discussion

We implemented this calibration method in C++ and tested it on a simulated model of a 6 DOF Titan 4 manipulator arm. With no measurement noise, the optimizer converged to a solution that resulted in <1mm end-effector accuracy, regardless of the initial parameter error. However, with added measurement noise as little as 1cm, the solution resulted in an end-effector accuracy of 5-15cm, which is unacceptable for most manipulation tasks. The issues with this optimizer are illustrated in Figure 3.

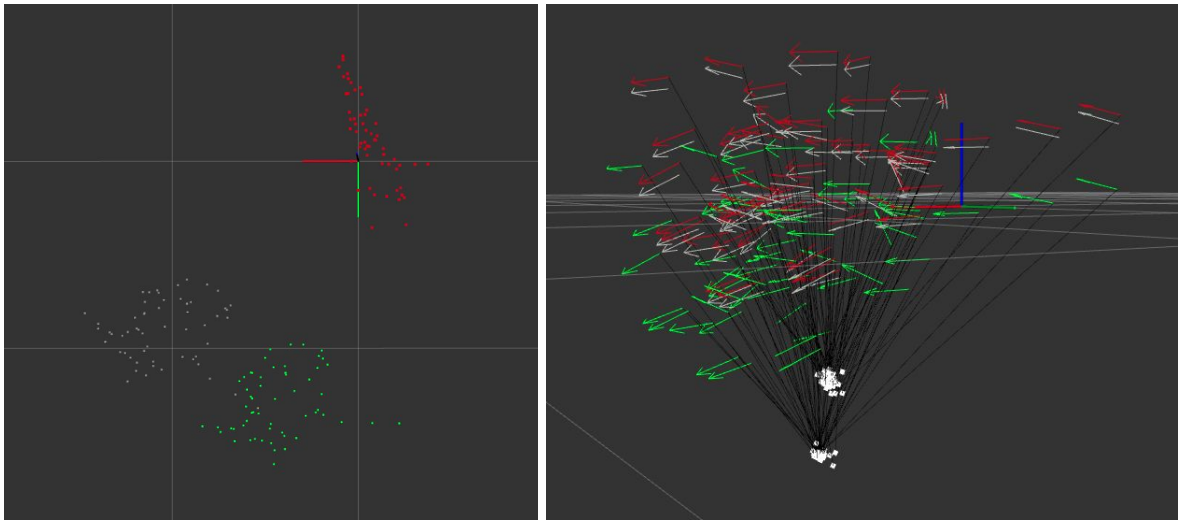

Figure 3: (Left) While the optimized end-effector positions (green) are much closer to the ground-truth positions (grey) than the uncalibrated positions (red), the position error is still quite high. (Right) When the initial parameters are very close to the correct values, the optimizer finds a solution that results in less variance between the projected measurements (in white) but a much higher end-effector error.

To gain some insight as to why this is the case, we ran a sensitivity test on the optimizer. In 5 degree increments from 0 to 180, an error was applied to each of the individual joints, and the resulting impact of that addition on the objective function and the end-effector error were computed. The results of this test are displayed in Figure 4

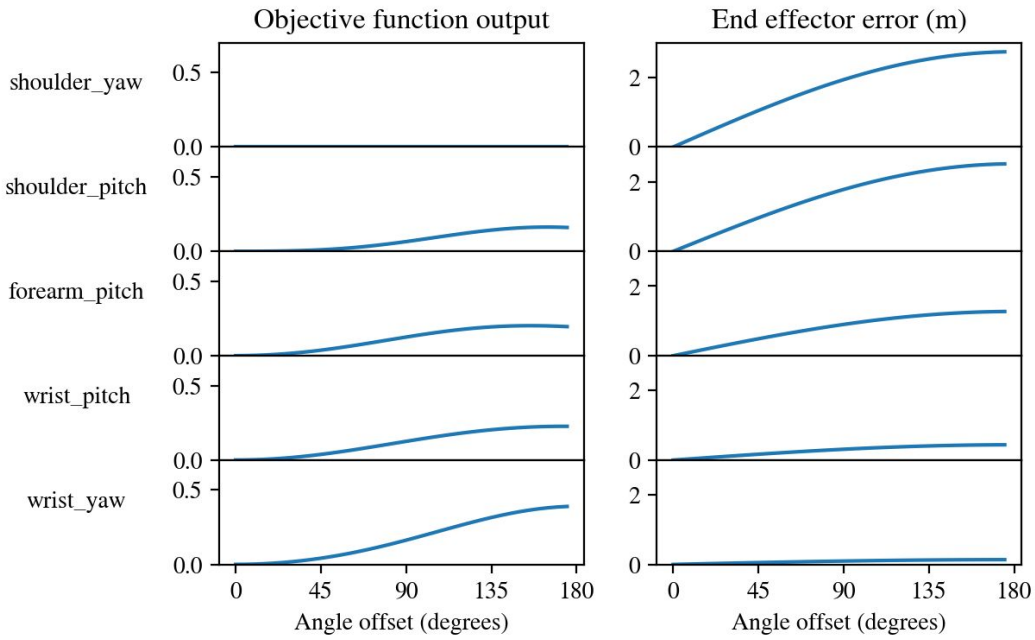

Figure 4: Results from adding an angle offset to each individual joint plotted against the corresponding output from the minimum variance objective function and the impact on end-effector error.

Looking at Figure 4, we can see that even at relatively high levels of joint error (~25 degrees), the objective function still outputs values quite close to 0; meanwhile, at 25 degrees, the end-effector error is quite high, up to ~75cm. To make matters worse, errors in joints lower in the kinematic chain (i.e. the shoulder) have a lower effect on the objective function output, but have a significantly higher effect on the resulting end-effector error.

These issues provide a likely explanation as to why the objective function converges perfectly when there is no measurement noise but will converge to rather inaccurate solutions with the slightest bit of measurement noise. With measurement noise, the minimum value of the objective function becomes obfuscated, resulting in inaccurate solutions that cannot be used in practice. These unfavorable results drive us to seek out another solution to the calibration problem.

The Proposed Method

Objective Function

Our proposed method uses the same formulation to describe the linear relationship between the joint sensor and angle, which is summarized by equation 2.

Using the same notation as before, each calibration data point ${}^{c}\mathbf{z}_{ij}$ consists of a 3D position of a landmark with respect to the wrist camera frame. ${}^{b}\mathbf{z}_{ij}$ are the computed positions of the points with respect to the base frame based on $\mathbf{k}_1$ and $\mathbf{k}_2$. To extend the previous definitions, we'll additionally define ${}^{b}\hat{\mathbf{z}}_{j}$ as the known 3D position of landmark j with respect to the base frame.

For each landmark, we compute the total sum of distances between ${}^{b}\mathbf{z}_{ij}$ and ${}^{b}\hat{\mathbf{z}}_{j}$. Our objective function can be represented by the equation:

$$\mathbf{v}^{\star} = \arg\min_{\mathbf{v}} \left(\sum_{j=1}^{n} \sum_{i=1}^{m} \sqrt{\left({}^{b}\mathbf{z}_{ij_x} - {}^{b}\hat{\mathbf{z}}_{j_x}\right)^2 + \left({}^{b}\mathbf{z}_{ij_y} - {}^{b}\hat{\mathbf{z}}_{j_y}\right)^2 + \left({}^{b}\mathbf{z}_{ij_z} - {}^{b}\hat{\mathbf{z}}_{j_z}\right)^2} \right)$$

where n is the number of landmarks and m is the number of calibration points per landmark

In other words, the solution to our optimization problem is the set of free parameters that would minimize the sum of distances between the measurements when transformed through the kinematic chain to the base frame and the known landmark position.

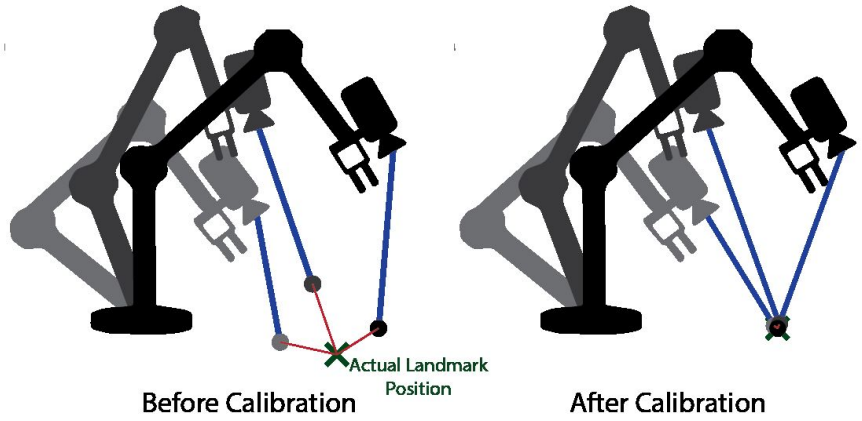

Figure 5: Minimum distance method visualization - the minimum distance method minimizes the distance between the reprojected observations and the known position of the landmark in the base frame

Calibration Process

The calibration process can be broken up into two primary parts: data collection and optimization. The diagram shown in Figure 6 provides a detailed breakdown of these two processes.

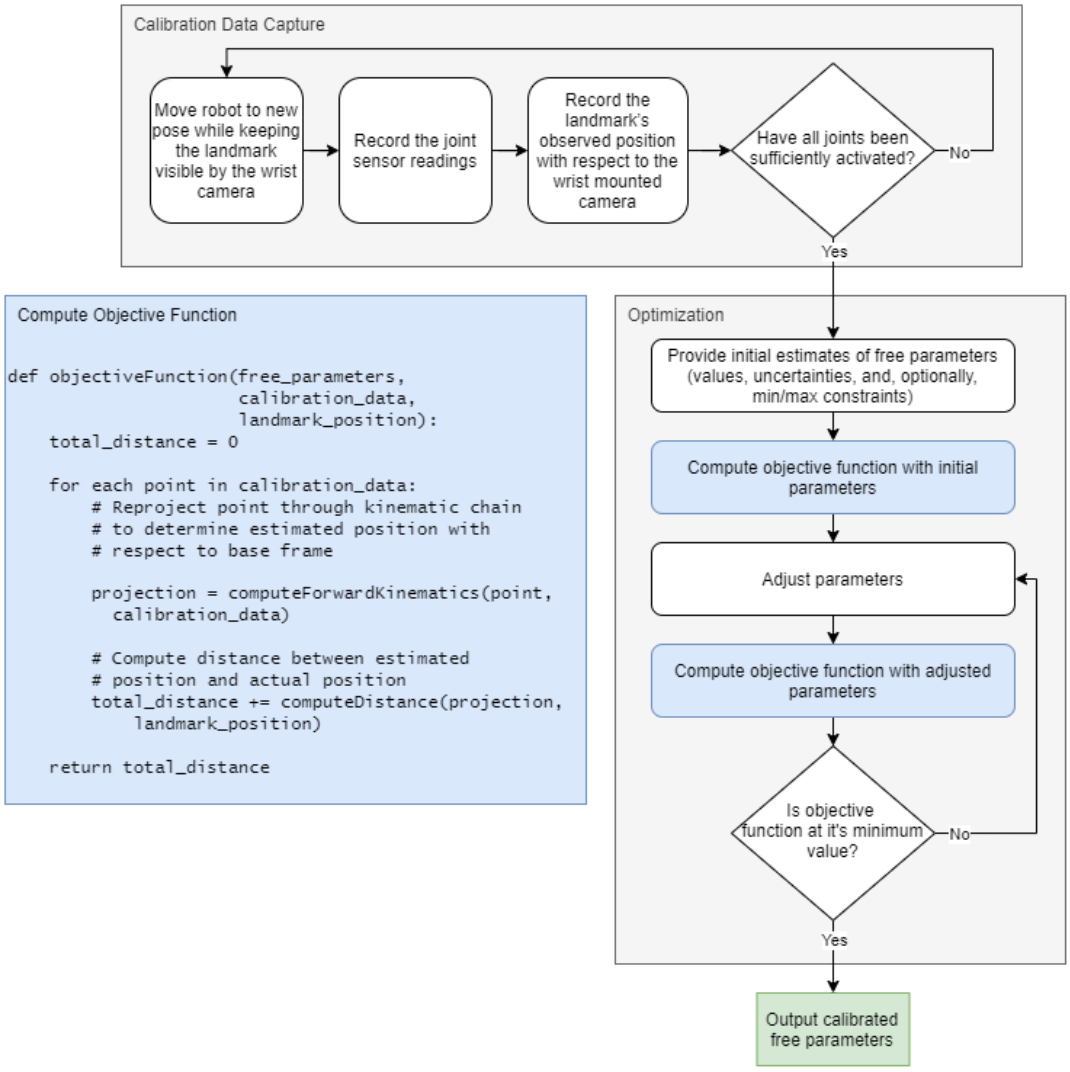

Figure 6: High-level overview of calibration process. Calibration happens in two primary steps - data capture and optimization. During the optimization step, the objective function is computed and the free parameters are adjusted to optimal values.

Analysis & Discussion

Like the minimum variance method, we also implemented this calibration method in C++ and tested it on a simulated model of a 6 DOF Titan 4 manipulator arm. The results looked much more promising, with the optimizer converging to a solution with <1mm end-effector error with or without measurement uncertainty. This can be explained by the strong response of the objective function to errors within joint angles, which is illustrated by the results of the sensitivity test presented in Figure 7.

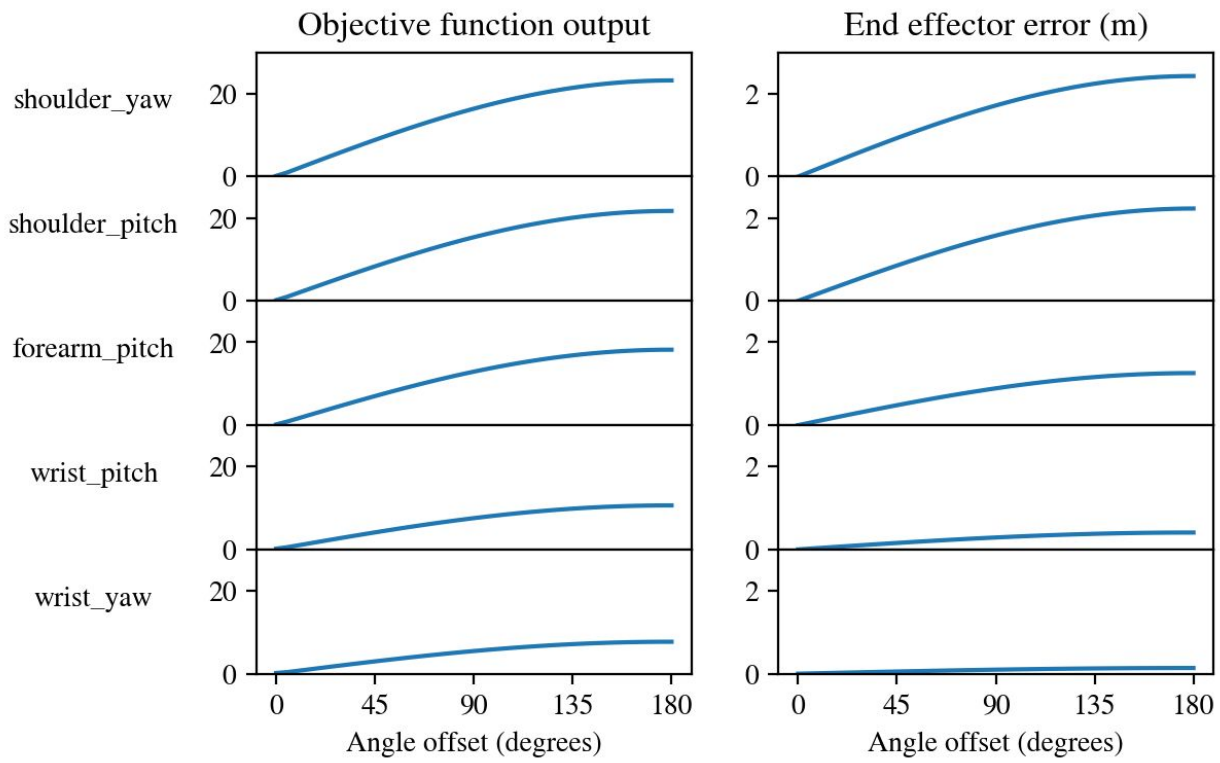

Figure 7: Results from adding an angle offset to each individual joint plotted against the corresponding output from the minimum distance objective function and the impact on end-effector error.

Conclusion

While appealing since it has fewer requirements, the Minimum Variance method is not viable for calibration due to its extreme sensitivity to measurement uncertainty, as the sensitivity tests show. The proposed Minimum Distance method is substantially more robust while only needing one more requirement than the Minimum Variance method, which makes it more practical for real-life calibration tasks. The proposed calibration method can be done in-situ, and is extensible to recalibration even with failed joints, which makes it an improvement over existing methods for remote underwater applications.

Figure 8: Testbed setup - a 6 degree-of-freedom hydraulic Kraft manipulator arm with a calibrated wrist-mounted fisheye camera and Apriltag fiducials on the base and in the environment

References

[1] Satja Sivčev, Joseph Coleman, Edin Omerdić, Gerard Dooly, Daniel Toal, Underwater manipulators: A review, Ocean Engineering, Volume 163, 2018, Pages 431-450, ISSN 0029-8018, https://doi.org/10.1016/j.oceaneng.2018.06.018. (http://www.sciencedirect.com/science/article/pii/S0029801818310308)

[2] A. D. Bowen et al., "Design of Nereid-UI: A remotely operated underwater vehicle for oceanographic access under ice," 2014 Oceans - St. John's, St. John's, NL, 2014, pp. 1-6, doi: 10.1109/OCEANS.2014.7003125.

[3] H.H. Roberts, W. Shedd, J. Hunt, Dive site geology: DSV ALVIN (2006) and ROV JASON II (2007) dives to the middle-lower continental slope, northern Gulf of Mexico, Deep Sea Research Part II: Topical Studies in Oceanography, Volume 57, Issues 21–23, 2010, Pages 1837-1858, ISSN 0967-0645, https://doi.org/10.1016/j.dsr2.2010.09.001. (http://www.sciencedirect.com/science/article/pii/S0967064510002481)

[4] M. Cai, Y. Wang, S. Wang, R. Wang, Y. Ren and M. Tan, "Grasping Marine Products With Hybrid-Driven Underwater Vehicle-Manipulator System," in IEEE Transactions on Automation Science and Engineering, vol. 17, no. 3, pp. 1443-1454, July 2020, doi: 10.1109/TASE.2019.2957782.

[5] Hai Huang, Qirong Tang, Jiyong Li, Wanli Zhang, Xuan Bao, Haitao Zhu, Gang Wang, A review on underwater autonomous environmental perception and target grasp, the challenge of robotic organism capture, Ocean Engineering, Volume 195, 2020, 106644, ISSN 0029-8018,

https://doi.org/10.1016/j.oceaneng.2019.106644.
(http://www.sciencedirect.com/science/article/pii/S0029801819307644)

[6] Vogt DM, Becker KP, Phillips BT, Graule MA, Rotjan RD, et al. (2018) Shipboard design and fabrication of custom 3D-printed soft robotic manipulators for the investigation of delicate deep-sea organisms. PLOS ONE 13(8): e0200386. https://doi.org/10.1371/journal.pone.0200386

[7] G. Meinecke, V. Ratmeyer and J. Renken, "HYBRID-ROV - Development of a new underwater vehicle for high-risk areas," OCEANS'11 MTS/IEEE KONA, Waikoloa, HI, 2011, pp. 1-6, doi: 10.23919/OCEANS.2011.6106913.

[8] NOAA: How much of the ocean have we explored?. National Ocean Service website, https://oceanservice.noaa.gov/facts/exploration.html#:~:text=More%20than%20eighty%20percent%20of,the%20mysteries%20of%20the%20deep, accessed on 9/7/2020.

[9] Q. Tian et al., "Influence of Ambient Pressure on Performance of a Deep-sea Hydraulic Manipulator," OCEANS 2019 - Marseille, Marseille, France, 2019, pp. 1-6, doi: 10.1109/OCEANSE.2019.8867485

[10] H. Nayar et al., "Long reach sampling for ocean worlds," 2017 IEEE Aerospace Conference, Big Sky, MT, 2017, pp. 1-7, doi: 10.1109/AERO.2017.7943680.

[11] Mooring, B. & Roth, Zvi & Driels, M.. (1991). Fundamentals of Manipulator Calibration.

[12] Marko Švaco, Bojan Šekoranja, Filip Šuligoj, Bojan Jerbić, Calibration of an Industrial Robot Using a Stereo Vision System, Procedia Engineering, Volume 69, 2014, Pages 459-463, ISSN 1877-7058, https://doi.org/10.1016/j.proeng.2014.03.012.
(http://www.sciencedirect.com/science/article/pii/S1877705814002586)

[13] Bingtuan Gao, Yong Liu, Ning Xi, Yantao Shen, "Developing an Efficient Calibration System for Joint Offset of Industrial Robots", Journal of Applied Mathematics, vol. 2014, Article ID 769343, 9 pages, 2014. https://doi.org/10.1155/2014/769343

[14] Y. Liu et al., "Development and sensitivity analysis of a portable calibration system for joint offset of industrial robot," 2009 IEEE/RSJ International Conference on Intelligent Robots and Systems, St. Louis, MO, 2009, pp. 3838-3843, doi: 10.1109/IROS.2009.5353951.

[15] Du, Biqiang & Xi, Ning & Nieves, Erick. (2012). Industrial robot calibration using a virtual linear constraint. International Journal on Smart Sensing and Intelligent Systems. 5. 987-1001. 10.21307/ijssis-2017-519.

[16] Heping Chen, T. Fuhlbrigge, Sang Choi, Jianjun Wang and Xiongzi Li, "Practical industrial robot zero offset calibration," 2008 IEEE International Conference on Automation Science and Engineering, Arlington, VA, 2008, pp. 516-521, doi: 10.1109/COASE.2008.4626417.

[17] W. S. Newman, C. E. Birkhimer, R. J. Horning and A. T. Wilkey, "Calibration of a Motoman P8 robot based on laser tracking," Proceedings 2000 ICRA. Millennium Conference. IEEE International Conference on Robotics and Automation. Symposia Proceedings (Cat. No.00CH37065), San Francisco, CA, USA, 2000, pp. 3597-3602 vol.4, doi: 10.1109/ROBOT.2000.845292.

[18] Y. Choi, J. Cheong, J. H. Kyung and H. M. Do, "Zero-offset calibration using a screw theory," 2016 13th International Conference on Ubiquitous Robots and Ambient Intelligence (URAI), Xi'an, 2016, pp. 526-528, doi: 10.1109/URAI.2016.7625770.

[19] Hanqi Zhuang, S. H. Motaghedi and Z. S. Roth, "Robot calibration with planar constraints," Proceedings 1999 IEEE International Conference on Robotics and Automation (Cat. No.99CH36288C), Detroit, MI, USA, 1999, pp. 805-810 vol.1, doi: 10.1109/ROBOT.1999.770073.

[20] T. S. Lembono, F. Suárez-Ruiz and Q. Pham, "SCALAR - Simultaneous Calibration of 2D Laser and Robot's Kinematic Parameters Using Three Planar Constraints," 2018 IEEE/RSJ International Conference on Intelligent Robots and Systems (IROS), Madrid, 2018, pp. 5570-5575, doi: 10.1109/IROS.2018.8594073.

[21] Lind, Morten. (2012). Automatic Robot Joint Offset Calibration.

[22] José Maurício S.T. Motta, Guilherme C. de Carvalho, R.S. McMaster, Robot calibration using a 3D vision-based measurement system with a single camera, Robotics and Computer-Integrated Manufacturing, Volume 17, Issue 6, 2001, Pages 487-497, ISSN 0736-5845, https://doi.org/10.1016/S0736-5845(01)00024-2. (http://www.sciencedirect.com/science/article/pii/S0736584501000242)

[23] F. Ghassemi, S. Tafazoli, P. D. Lawrence and K. Hashtrudi-Zaad, "Design and Calibration of an Integration-Free Accelerometer-Based Joint-Angle Sensor," in IEEE Transactions on Instrumentation and Measurement, vol. 57, no. 1, pp. 150-159, Jan. 2008, doi: 10.1109/TIM.2007.904488.

[24] L. Cantelli, G. Muscato, M. Nunnari and D. Spina, "A Joint-Angle Estimation Method for Industrial Manipulators Using Inertial Sensors," in IEEE/ASME Transactions on Mechatronics, vol. 20, no. 5, pp. 2486-2495, Oct. 2015, doi: 10.1109/TMECH.2014.2385940.

[25] X. Xu, Y. Sun, X. Tian and L. Zhou, "A Novel Joint Angle Estimation Method for Serial Manipulator Using Micro-Electromechanical Systems Sensors," in IEEE Transactions on

Industrial Electronics, vol. 67, no. 12, pp. 10610-10620, Dec. 2020, doi: 10.1109/TIE.2019.2962442.

[26] H. T. Butt, M. Pancholi, M. Musahl, P. Murthy, M. A. Sanchez and D. Stricker, "Inertial Motion Capture Using Adaptive Sensor Fusion and Joint Angle Drift Correction," 2019 22th International Conference on Information Fusion (FUSION), Ottawa, ON, Canada, 2019, pp. 1-8.

[27] Pradeep V., Konolige K., Berger E. (2014) Calibrating a Multi-arm Multi-sensor Robot: A Bundle Adjustment Approach. In: Khatib O., Kumar V., Sukhatme G. (eds) Experimental Robotics. Springer Tracts in Advanced Robotics, vol 79. Springer, Berlin, Heidelberg. https://doi.org/10.1007/978-3-642-28572-1_15

[28] Q. V. Le and A. Y. Ng, "Joint calibration of multiple sensors," 2009 IEEE/RSJ International Conference on Intelligent Robots and Systems, St. Louis, MO, 2009, pp. 3651-3658, doi: 10.1109/IROS.2009.5354272.

[29] Wise, M., Michael Ferguson, Daniel King, Eric Diehr and David Dymesich. “Fetch & Freight : Standard Platforms for Service Robot Applications.” (2016).

[30] Garcia, C. Fully Vision-based Calibration of a Hand-Eye Robot. Autonomous Robots 6, 223–238 (1999). https://doi.org/10.1023/A:1008891612854

[31] J. M. Hollerbach and D. M. Lokhorst, "Closed-loop kinematic calibration of the RSI 6-DOF hand controller," in IEEE Transactions on Robotics and Automation, vol. 11, no. 3, pp. 352-359, June 1995, doi: 10.1109/70.388777.

[32] NOAA, “Seven miles deep, the ocean is still a noisy place”. National Ocean Service website, https://www.noaa.gov/media-release/seven-miles-deep-ocean-is-still-noisy-place, accessed on 9/7/2020.

[33] NOAA, “How does the temperature of ocean water vary?”. National Ocean Service website, https://oceanexplorer.noaa.gov/facts/temp-vary.html, accessed on 9/7/2020.

[34] R. L. Williams. Kinematics of the Six-degree-of-freedom Force-reflecting Kraft Master. Tech. rep. Hampton, VA, United States: NASA Langley Research Center, 1991.

[35] Tingfan Wu, Y. Tassa, V. Kumar, J. Movellan and E. Todorov, "STAC: Simultaneous tracking and calibration," 2013 13th IEEE-RAS International Conference on Humanoid Robots (Humanoids), Atlanta, GA, 2013, pp. 469-476, doi: 10.1109/HUMANOIDS.2013.7030016.

[36] Donghai Ma, J. M. Hollerbach and Yangming Xu, "Gravity based autonomous calibration for robot manipulators," Proceedings of the 1994 IEEE International Conference on Robotics and Automation, San Diego, CA, USA, 1994, pp. 2763-2768 vol.4, doi: 10.1109/ROBOT.1994.350919.

[37] Bernd Pfrommer, & Kostas Daniilidis. (2019). TagSLAM: Robust SLAM with Fiducial Markers.

[38] S. Kim et al., "Robot Head-Eye calibration using the Minimum Variance method," 2010 IEEE International Conference on Robotics and Biomimetics, Tianjin, 2010, pp. 1446-1451, doi: 10.1109/ROBIO.2010.5723542.